Enzymatic reduction of CO2 to formic acid using FDH immobilized on natural zeolite

Enzymatic reduction of CO_2 to formic acid using FDH immobilized on natural zeolite

Giuseppe Pietricola[1], Carminna Ottone[2*], Debora Fino[1], Tonia Tommasi[1*]

[1]Department of Applied Science and Technology, Politecnico di Torino,

Corso Duca degli Abruzzi 24, 10129, Turin, Italy

[2]Escuela de Ingeniería Bioquímica, Pontificia Universidad Católica de Valparaíso, Av. Brasil 2085, Valparaíso, Chile

*Corresponding authors

E-mail addresses: carminna.ottone@pucv.cl (C. Ottone), tonia.tommasi@polito.it (T. Tommasi)

Abstract

The enzymatic strategy for methanol production starting from CO_2 involves the use of three enzymes in series. The first enzyme of the series, which reduces CO_2 to formic acid, is formate dehydrogenase (FDH). A problem with using free enzymes is their low stability. To overcome this limitation, the use of immobilized enzymes has been extensively studied in literature. In particular, porous supports such as silica or zeolite have been widely examined for covalent immobilization.

This work presents a strategy of immobilization of the NADH dependent FDH from *C. boidinii* on natural zeolite to study the CO_2 reduction reaction to formic acid. The support functionalization was carried out with glyoxyl (Z_G) or amino (Z_A) groups, to covalently bind the enzyme to the support. To carry out a covalent immobilization with Z_A, glutaraldehyde was added after the ionic bond between the enzyme and the support. The samples were evaluated in terms of specific activity, immobilization yields and thermal stability. As a whole, the covalently immobilized enzyme exhibited higher thermal stability than the free enzyme, with a stability factor of ~15 with Z_G and ~19 with Z_A. Finally, FDH immobilized on Z_G and Z_A supports were tested for the production of formic acid in a CO_2 saturated medium. The conversion, referred to NADH, was equal to 37 % with Z_A and 34.6 % with Z_G. Finally, the reusability of the biocatalysts was studied. The residual activity after 12 cycles was 80% and 22% with Z_G and Z_A, respectively.

Graphical abstract

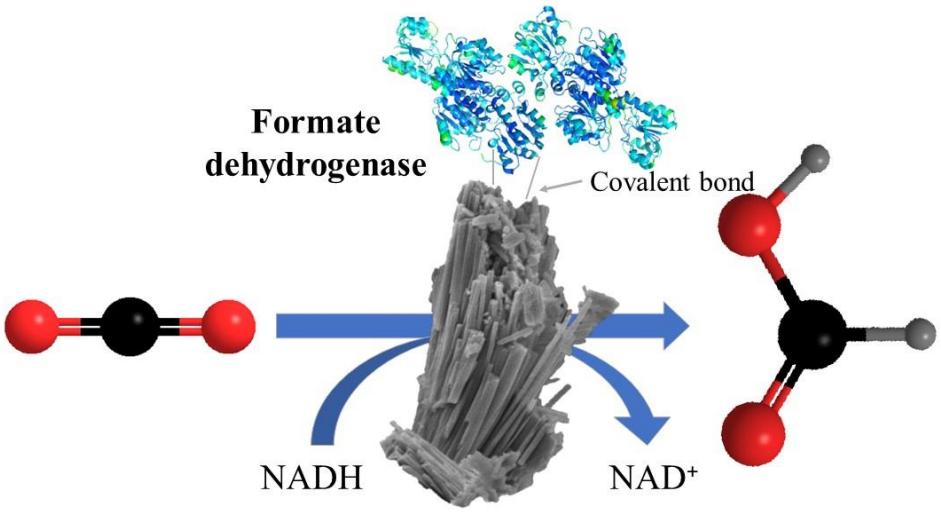

1 Introduction

During 2016 the concentration of carbon dioxide in the atmosphere exceeded the threshold of 400 ppm, throughout the whole year. This threshold is defined as the point of no return [1]. As a result, CO_2 capture and utilization systems are increasingly being studied. Currently, there is no technology that can be used on a large scale for the conversion of CO_2. Some of the most studied methods of CO_2 reduction are heterogeneous, photocatalytic, electrochemical and microbial catalysis, with which it is possible to obtain products of great interest such as CO, formic acid, methane and methanol [2–5].

A further promising strategy is enzymatic reduction. Although productivity with this system is not particularly high, enzymatic reduction is an interesting strategy because it allows a high selectivity of CO_2 and thus making it possible to work at ambient temperature and pressure. The products obtainable from enzyme catalysis are the same as those that can be obtained from the other reduction processes, which will depend on the selection of the involved enzymes [2]. A process of great interest is methanol production using three enzymes in series. The first reaction is catalyzed by the enzyme formate dehydrogenase (FDH) which reduces the CO_2 to formic acid. Subsequently, formaldehyde dehydrogenase ($F_{ald}DH$) produces formaldehyde from formic acid and finally alcohol dehydrogenase (ADH) reduces formaldehyde to methanol which can be used directly as a fuel or as a starting point for many basic chemical reactions [3,6,7].

In recent years it has been increasingly studied for the CO_2 conversion reaction [2,8–10]. In the reaction of CO_2 reduction, FDH requires nicotinamide adenine dinucleotide in the reduced form (NADH) as cofactor, as shown in Figure 1. The dependence of these enzymes on this molecule has been a limitation for the development of new technologies with dehydrogenases due to the high cost of the cofactor, which is associated with the production and purification process. However, in the literature there are various emerging techniques such as chemical, enzymatic, electrocatalytic and photocatalytic regeneration methods that would make it possible to overcome this issue, increase the productivity of the target reaction and to work in a continuous system mode [9,11,12].

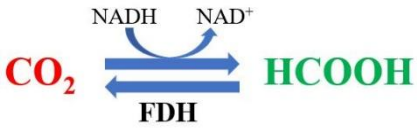

Figure 1 – Conversion of CO_2 to formic acid catalyzed with formate dehydrogenase (FDH)

As shown in Figure 1, the reaction catalyzed by FDH is reversible. Several studies are focused on finding the FDH source that shows the highest activity toward the reduction reaction. The most effective enzyme in reducing CO_2 reported so far is FDH from *Thiobacillus* sp. [13]. However, the vast majority of the studies found in literature use FDH from *Candida boidinii* for the CO_2 reduction reaction due to its higher commercial availability even if the oxidation activity is higher than that of the reduction activity.

A further problem using enzymes is their low stability. To overcome this limitation, the use of immobilized enzymes has been studied in the literature. Moreover, thanks to immobilization, the biocatalyst is easily separated from the final product of interest and can be reused for a new cycle [14]. By comparing covalent and ionic immobilization strategies, different studies have reported that highest immobilization yields are obtained with ionic adsorption but at the expense of the stability. However, the use of covalent immobilization makes it possible to obtain a good compromised between thermal stability and retained activity [15]. The same result was confirmed by Bolivar et al. by using agarose particles activated with different functional groups as support in the immobilization of FDH from *C. boidinii* [16]. By using amino activated supports a covalent bonding can be obtained by adding glutaraldehyde, this is a bifunctional molecule that react with the amino groups of the lysine residues and the amino groups of the support. The covalent bond with glutaraldehyde can be performed in two forms: (i) before the

immobilization by activating the amino functionalized supports or (ii) after the ionic immobilization to avoid enzyme leakage. López-Gallego et al. demonstrated that between these two strategies, the treatment of the adsorbed enzymes with glutaraldehyde yields to a higher stabilization factor with respect to the use of a pre-activated support [17]. In addition, the subsequent addition of glutaraldehyde could have also a stabilizing effect by cross-linking the two subunits of multimeric enzymes, similarly to that reported with polymeric cross-linkers [18]. Despite ionic polymers higher concentrations of glutaraldehyde could also yield to a rigidification of the protein, which is observed in a lower retained activity [19].

Some of the most studied materials for carrying out a covalent immobilization are agarose [20], chitosan [21], mesoporous silica [22] and zeolite [23–25]. However, the use of zeolite as support for the FDH enzyme has not been reported so far. Zeolite is a hierarchical mesoporous material with a high surface area that can be found in nature or can be produced artificially by means of different preparation procedures [26,27]. The use of natural zeolite is very relevant because it is possible to obtain a significant increase in thermal and mechanical stability with a very low cost in raw materials. Another advantage of this material, is that zeolite is a very versatile material, similar to silica, and its surface can be modified with several functional groups [23].

This work presents a biocatalyst made of an FDH immobilized on natural zeolites for the reaction of production of formic acid from carbon dioxide. Different immobilization methods were studied and untreated and functionalized zeolites with amino and glyoxyl groups were used. The physicochemical properties of the zeolite were characterized by FTIR, XRD and FESEM analyses. Moreover, the thermal stability of the immobilized enzyme was evaluated and compared with the free enzyme, as well as the temperature, pH profile and operational stability of the different biocatalysts.

In this work, FDH form *Candida boidinii* was selected due to its greater availability. However, this work gives a choice of low-cost support and immobilization procedure that can be replicated with FDH from other sources.

2 Materials and methods

2.1 Materials

(3-Glycidyloxypropyl)trimethoxysilane (GPTMS, ≥98%), (3-Aminopropyl)triethoxysilane (APTES, ≥98%), sulfuric acid (≥98%), sodium borohydride (≥98%) were purchased from Sigma-Aldrich. Sodium metaperiodate, glycerol, glutaraldehyde (25%), sodium formate were supplied from Merck. Formate dehydrogenase (FDH) from *Candida boidinii* with a protein concentration of 43

± 1 mg/ml (according to Bradford assay [28]) was purchased from Megazyme. NAD^+ (99.6%) and NADH (97.1%) were supplied from GERBU Biotechnik and natural zeolite (Z) was obtained from Minera Formas (Chile).

2.2. Zeolite activated with glyoxyl groups (Z_G)

The modification with glyoxyl groups was carried out with three reactions in series, as modified from literature [22]. For the generation of epoxy groups 1.0 g of support is put in contact with a GPTMS solution (5% v/v in toluene) at 105 °C for 5 h under vigorous stirring in a balloon with a cooling column. After filtration and washing with acetone and distilled water, the epoxy group hydrolysis is carried out using a 0.1 M H_2SO_4 solution for 2 h at 85 °C under stirring in a balloon with a cooling column. After filtrating and washing with distilled water, an oxidation is carried out using a 0.1 M $NaIO_4$ solution at room temperature for 2 h to finally obtain glyoxyl groups. Subsequently, the support was filtrated and washed with distilled water/phosphate buffer 0.1 M pH 7.5 and dried at room temperature. The volume of the three solutions used was equal to 30 ml. The moles of glyoxyl groups generated were quantified by back titration with $NaHCO_3$/KI, as described by Guisan [29]. The absorbance of the supernatant at 405 nm before and after the oxidation process, carried out with $NaIO_4$, was measured and related to the glyoxyl groups produced. The content of glyoxyl groups of the Z_G samples was equal to 375 $\mu mol/g_{support.}$

2.3 Zeolite activated with amino groups (Z_A)

For the generation of amino groups 1.0 g of support was put in contact with 30 ml of APTES solution (5% v/v in toluene) at 105 °C for 5 h in a balloon with a cooling column under strong stirring. The protocol was modified from literature [30]. After filtration and washing with acetone, distilled water and phosphate buffer 0.1 M pH 7.5, the support was dried at room temperature.

2.4 Characterization of supports

An x-ray diffraction (XRD) analysis was performed to characterize the structure of the zeolite. The XRD spectrum was obtained with a Philips PW3040 X'Pert diffractometer, using Cu Kα radiation (2θ range = 5°–50°; step = 0.013° 2θ). The diffraction peaks were assigned according to the Powder Data File database (PDF 2004, International Centre of Diffraction Data, Pennsylvania).

FTIR spectra were obtained using a Jasco FT/IR-4600 spectrophotometer with an ATR module at room temperature over the range of 4000-600 cm^{-1} with a resolution of 2 cm^{-1} and using a number of scan equal to 64. The functions of noise elimination, H_2O and CO_2 reduction and auto baseline correction have been used.

The specific surface area (S_{BET}) of zeolite was calculated using the Brunauer–Emmett–Teller method via N_2 physisorption at 77K with a Micromeritics TriStar II 3020 instrument. The pore volume (V_T) and pore diameter (D_p) were estimated with the Barrett-Joyner-Halenda method, during the desorption phase. Before the analysis, the samples were outgassed at 200 °C for 2h.

The morphology of the zeolite samples was observed with a field emission scanning electron microscope (FESEM Zeiss MERLIN, Gemini-II column).

2.5 Enzymatic activity assay

A solution consisting of 2.3 ml of phosphate buffer 100 mM pH 7.5, 0.5 ml of sodium formate 300 mM, 0.1 ml of NAD^+ 50 mM was used. Then 0.1 ml of commercial FDH solution with a 1:100 dilution (for the activity of the free enzyme) or 10 mg of support (for the activity of the immobilized enzyme) was added. A milling process on zeolite with a mortar was carried out to measure the activity of the immobilized enzyme. The change in absorbance at 340 nm dependent on the formation of NADH, which is generated during the oxidation of formate, is measured using a Jasco V-730 UV-visible spectrophotometer. The activity is expressed in IU (international units) and corresponds to the amount of enzyme necessary to produce one µmol/min of NADH at pH 7.5 and 30 °C. The specific activity is the activity referred to the amount of enzyme in solution in the case of the free enzyme or to the quantity of support in the case of immobilized enzyme.

2.6 Immobilization of the enzyme

For the immobilization of FDH, three different support were studied, the untreated zeolite (Z) and the zeolites activated with glyoxyl (Z_G) or amino groups (Z_A). In addition, the immobilization with the three supports was performed with both the as made and milled samples (Z_m). The milling was performed with a mortar. Generally, 30 mL of a solution containing 2 mg of FDH was put in contact with 1 g of support for 5 h. In the course of the immobilization process, samples of supernatants were taken to perform the activity assay and the quantification of the protein concentration with the Bradford assay [28]. In order to control the stability of the soluble enzyme at the immobilization conditions, the enzyme activity of a blank, without support, was measured during the immobilization. FDH was immobilized on functionalized and non-functionalized zeolite. The immobilization yield (IY) was obtained from the difference of the mass of enzyme protein in the immobilization solution between the beginning ($m_{E,t0}$) and the end ($m_{E,tf}$) of the process, as expressed in equation (1).

$$IY = \frac{m_{E,t_0} - m_{E,t_f}}{m_{E,t_0}} \quad (1)$$

The immobilization was also evaluated according to the retained activity (R_{act}), which is calculated as the division of the specific activity of the biocatalyst (A_{IE} in $IU \cdot g_{support}^{-1}$) by the contacted activity (C_{act}), as expressed in equation (2). C_{act} represent the maximum specific activity that the support would show, if all the contacted protein was immobilized and full active. C_{act} is calculated as the product of the initial enzyme load in the immobilization solution (q_E in $mg_{protein} \cdot g_{support}^{-1}$) per the specific activity of the free enzyme at time zero of the immobilization process ($A_{FE,\,t0}$ in $IU \cdot mg_{protein}^{-1}$):

$$R_{act} = \frac{A_{IE}}{q_E \cdot A_{FE,t_0}} \cdot 100 = \frac{A_{IE}}{C_{act}} \cdot 100 \quad (2)$$

To determine if the enzyme can be immobilized within the channels of the zeolite, the diameter of the enzyme was calculated by using the equation (3). This equation considered that the shape of the protein approximates to a sphere [31]. M represent the molecular weight of the enzyme in Da.

$$R_{min} = 0.066 \cdot M^{\frac{1}{3}} \quad (3)$$

2.6.1 Immobilization on non-functionalized support

Two different conditions were evaluated to carried out the immobilization with the non-functionalized support by incubating the zeolite in the enzymatic solution prepared in (i) a carbonate buffer 100 mM pH 10.05 solution or in (ii) a phosphate buffer 5 mM pH 7, at 4 °C under gently stirring. In this case there is no covalent bond, but the enzyme is adsorbed on the zeolite surface. After 5 h, the supports were separated from the solutions by filtration and were dried at 4 °C.

2.6.2 Immobilization on glyoxyl support

Immobilization with glyoxyl supports was carried out in a solution of carbonate buffer 100 mM pH 10.05, with 15% v/v of glycerol at 4 °C under gently stirring. After 5 h of reaction, sodium borohydride was added (0.5% v/v in the buffer solution) to stabilize the bond between the

support and the enzyme. Finally, a washing was carried out with distilled water/phosphate buffer 100 mM pH 7.5 and the support was dried at 4 °C. This method was adapted from literature [22].

2.6.3 Immobilization on amino support

Immobilization with amino supports was carried out in a solution of phosphate buffer 5 mM pH 7 at a temperature of 4 °C under gently stirring. After 5 h of incubation, the support was separated from the enzymatic solution and was added to a 0.1% v/v glutaraldehyde solution, prepared in 25 mM buffer solution pH 7, for 30 min at 4 °C. Finally, a washing was carried out with phosphate buffer 5 mM pH 7 and the support was dried at 4 °C. This method was adapted from procedure reported in literature [16,32].

2.2.6 Temperature and pH profile of FDH derivates

The influence of pH and temperature on the soluble and immobilized enzyme was carried out with the activity test as described in section 2.5. Modifications were made to the activity test to evaluate the influence of temperature, incubating the biocatalysts at the following temperatures: 30 °C, 40 °C, 50 °C and 60 °C with a fixed pH of 7.5. The influence of pH was carried out with the activity test keeping the T fixed at 30 °C and varying only the pH in the range of 6 and 9. A phosphate buffer was used for the solutions at pH 6, 7, 7.5 and 8, while a carbonate buffer for the solution at pH 9. The relative activities are expressed as a percentage of the maximum value obtained for each set of experiments.

2.2.7 Thermal stability

The free enzyme (with a dilution of 1:300 from the original commercial solution) and the support with the immobilized enzyme were incubated in a 100 mM phosphate buffer solution pH 7.5 at 50 °C. Activity (*A*) was measured at different times and expressed as percentage of the starting activity in both the cases. A first order deactivation model with no residual activity (equation (4)) and with residual activity (equation (5)) was used to describe the decrease in activity of the free enzyme and the immobilized enzymes, respectively. A_0 is the initial activity (IU), k_D is the deactivation constant (h^{-1}), t is the time (h), α is the ratio between the final and initial states of the enzyme [33].

The half-lifetime of the free ($t_{1/2\ FE}$) and immobilized enzyme ($t_{1/2\ IE}$) was calculated from the respective models and was used to determine the stabilization factor (F_S), as shown in equation (6) [34].

$$A = A_0 \cdot e^{-k_D \cdot t}; \quad (4)$$

$$A = A_0 \cdot [(1-\alpha) \cdot e^{-k_D \cdot t} + \alpha]; \quad (5)$$

$$F_S = \frac{t_{1/2\,IE}}{t_{1/2\,FE}} \quad (6)$$

2.2.8 CO_2 reduction

A 14 mM solution of NADH dissolved in a phosphate buffer was added in a sealed glass bottle. The biocatalyst was introduced and subsequently CO_2 was blown, for the all the duration of the test. The reaction was carried out at room temperature and pH 7. The concentration of NADH was measured spectrophotometrically at 340 nm. Formic acid was analyzed in a Jasco HPLC equipped with a Photometric Diode Array Detector (MD-4010), a quaternary pump (Jasco PU-4180-LPG) and autosampler (Jasco AS-4050), at 210 nm UV and using a C18 column (150mm x 4.6mm x 5µm, Sciences). Samples were eluted with H_2SO_4 5mM at a flow-rate of 0.6 mL/min. The processing and analysis of the results was made in the software Jasco Chromnav 2.0. Formic acid (HPLC grade) was used to determine the retention time and check the linear range of the measurements.

2.2.9 Reusability of the immobilized FDH

Several batch reactions were performed to study the reuse of the immobilized enzyme. A solution with $NaHCO_3$ 34mM and NADH 14mM in a phosphate buffer 0.1M at pH 7 was put in contact with the immobilized enzyme. After each batch, the immobilized enzyme was filtered and washed with distilled water. Subsequently, activity was measured at pH 7.5 and T = 30 °C, as described in section 2.5. Each batch had a duration of 1 h.

3 Results and discussions

3.1 Characterization of the free enzyme

The activity assay was performed on the commercial FDH from *C. boidinii*. The specific activity turns out to be 3.02 ± 0.1 IU/$mg_{protein}$. Replacing the reported molecular weight of the FDH enzyme of M=74000 Da [35] in equation (3), a diameter equal to D=5.54 nm was estimated.

3.2 Characterization of supports

With the XRD analysis, 2 phases were identified in the support: mordenite (M, card no: 00-049-0924) and quartz (Q, card no: 01-083-0539). The spectrum is presented in the figure 2-a. The predominant phase was identified with mordenite.

FTIR analyzes were performed on the support as it is (Z) and functionalized with amino (Z_A) or glyoxyl groups (Z_G), as can be observed in Fig. 2-b. From the curve of the Z sample, the transmittance peak at 780 and 1015 cm^{-1} correspond respectively to the symmetric and asymmetric vibration band of the T-O-T group (where T represents Si or Al) [25,36,37]. The transmittance bands between 600–780 cm^{-1} are attributed to exchangeable cations due to pseudo-crystallinic vibrations, which are typical reported with natural zeolites. The bands at 910 cm^{-1} and 875 cm^{-1} are associated with bending vibrations of Al^{3+} hydroxyl groups [38,39]. It is also present a peak around 1650 cm^{-1}, corresponding to the zeolitic water [40].

The intensities of the zeolitic bands observed with the Z_G sample were lower to those obtained with Z and Z_A samples. The latter is attributed to the acidic treatment performed during the glyoxyl functionalization process, which has reported to yield to decationisation, dealumination and loss of crystallinity [41].

For the Z_A sample the peak at around 3430 cm^{-1} corresponds to the stretching vibration of amino groups [36,37,42]. From the FTIR spectrum it was not possible to see a peak related to the glyoxyl group (expected at ~1715 cm^{-1}) probably because of the low glyoxyl content obtained per gram of zeolite (375 µmol/$g_{support.}$).

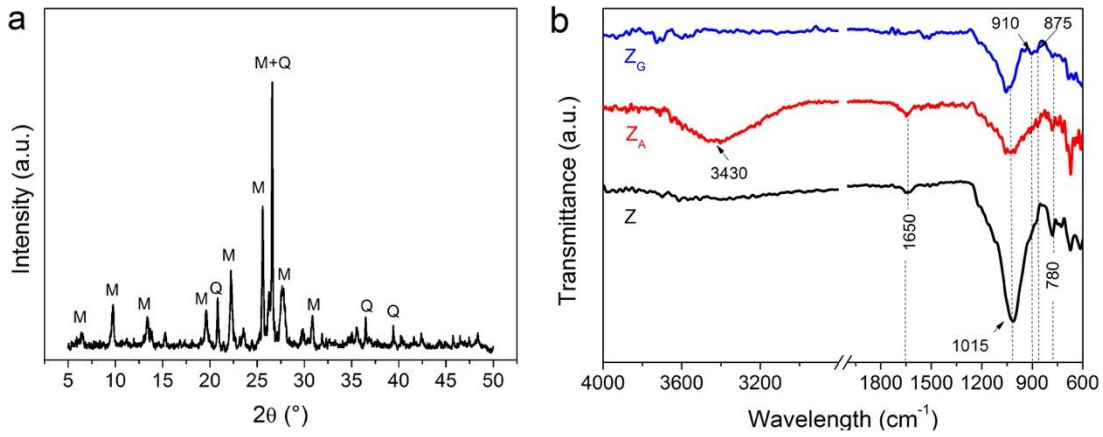

Figure 2 - (a) XRD spectrum of the untreated zeolite. (b) FTIR spectra of the untreated zeolite (Z) and of the zeolite functionalized with amino (Z_A) and glyoxyl (Z_G) groups.

Table 1 shows the results obtained by the nitrogen physisorption at 77K. In both the functionalized samples the BET surface area (S_{BET}) and total pore volume (V_T) decreased. S_{BET} corresponds to the sum of S_{micro} (specific surface of micropores) and S_{ext} (specific surface of meso and macropores). Using APTES, S_{BET} becomes about half of the untreated zeolite, probably because this molecule blocks smaller pores [43]. S_{ext} is very similar to the unmodified zeolite, while the surface decrease occurred with S_{micro}. Moreover, the volume of the micropores (V_{micro}) of the Z_A decreased by an order of magnitude. On the other hand, the volume of the larger pores (V_T-V_{micro}), is approximately constant. The pore average diameter (D_P) increased slightly in the Z_A, probably because the smaller pores have been occluded (data of pore distribution not shown). In the case of the Z_G, D_P decreased slightly due to the steric footprint of the GPTMS. In the three cases, the pore average diameter of the samples was greater than the diameter of the enzyme resulting from equation (3). So even after functionalization, it can be assumed that the enzyme was immobilized within the pores of the zeolite.

Table 1 - Surface area, pore volume and average mean diameter of the samples

Sample	BET surface area (S_{BET}) (m^2/g)	Micropore Area (S_{micro}) (m^2/g)	External surface area (S_{ext}) (m^2/g)	Total pore volume (V_T) (cm^3/g)	Micropore volume (V_{micro}) (cm^3/g)	Pore average diameter D_P (nm)
Z	72.55	52.22	20.33	0.078	0.027	13.55
Z_G	62.17	40.38	21.78	0.068	0.022	12.17
Z_A	29.19	10.87	18.32	0.053	0.003	14.75

The figure 3-a presents the typical channels with the diameter in the order of nm. The figure 3-b shows the distribution of zeolite particles after grinding. Particles ranging from tenths of a micrometer to a few micrometers are detectable.

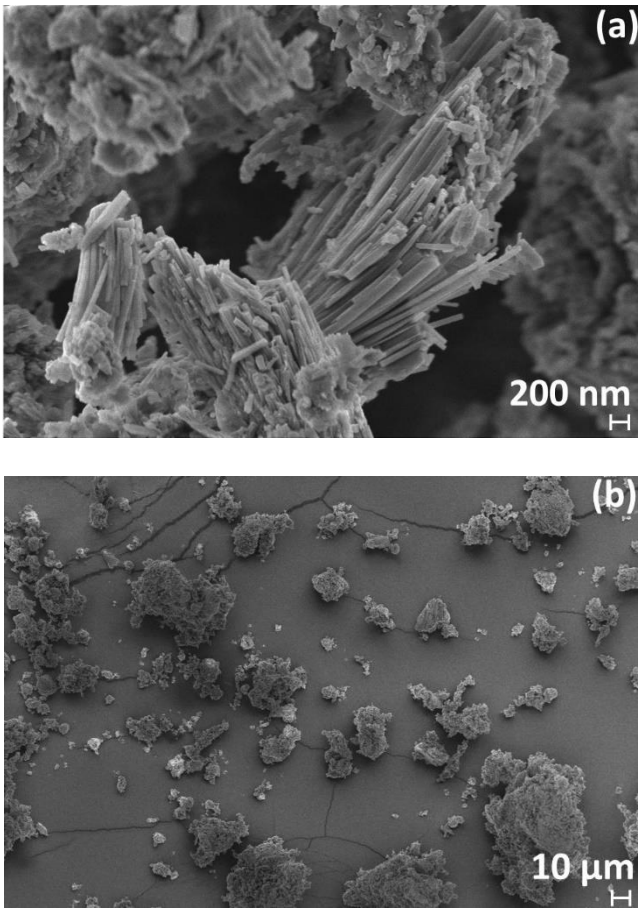

Figure 3 – FESEM images of (a) nanometric structure of the natural zeolite and of (b) zeolite particles after milling.

3.3 Characterization of the immobilized enzyme

Three different supports were studied for the immobilization of FDH, the zeolite as it is and two functionalized zeolites, Z_G and Z_A. On the one hand, the mechanism of immobilization of the non-functionalized zeolite was simple adsorption of the enzyme on the zeolite surface. On the other hand, the immobilization of FDH on the functionalized zeolites was covalently. In the case of Z_G, the covalent bonds occur due to the reaction of the amino groups of the lysine residues with the aldehyde groups of the support. In the case of Z_A, the immobilization mechanism was divided in two steps. In a first part, an ionic immobilization took place. Then, when the enzyme was already inside the support pores, a bifunctional crosslinker (i.e. glutaraldehyde) was added to permit a covalent bond between the lysine residues of the protein structure and the support or between two adjacent lysine residues.

Fig. 4 shows the kinetics of the immobilization processes with Z_G and Z_A, as exemplification mode, since the course of enzymatic activity was very similar in the various cases studied. In the case of Z_A, the kinetic presented (Fig. 4-b) corresponds only to the first immobilization step related

to ionic adsorption. Generally, as time passed, the activity of the supernatant decreased as the enzyme moved from the liquid phase (solution) to the solid phase (support). The activity of blank, thus, of the solution containing only the enzyme and not the support, remained constant during the whole process. The concentration of protein in solution was measured subsequently using the Bradford assay, from which it was therefore possible to derive the IY. The immobilization time was set at 5 h hours for all tests. For the Z_A samples, this time was considered for the immobilization step associated to the ionic bonding. In all cases there was a final activity of the supernatant lower than 40% of the initial activity. As can be seen in figure 4-a (Z_G), there was still 50% of protein in solution, with an activity of the supernatant lower than 10% of the initial activity. Instead, with Z_A the decrease in supernatant activity was similar to that of the protein in solution (fig. 4-b).

The differences of the immobilization rates observed between Z_G and Z_A were attributed both to the use of glycerol in the covalent immobilization and the ionic strength used in the case of ionic immobilization. The addition of glycerol for Z_G had the scope of protecting FDH from the damaging effect that has been reported for sodium borohydride with such enzyme, which was necessary to stabilize the covalent bond between the enzyme and the glyoxyl groups of the support [44]. However, the addition of glycerol reduced the mobility of the enzyme in the immobilization solution. In the case of Z_A, a high ionic strength was used during the immobilization, which was possible thanks to the low buffer concentration (5 mM) and the difference between the pH of immobilization solution (pH 7.0) and the isoelectric point of FDH (5.4, [45]).

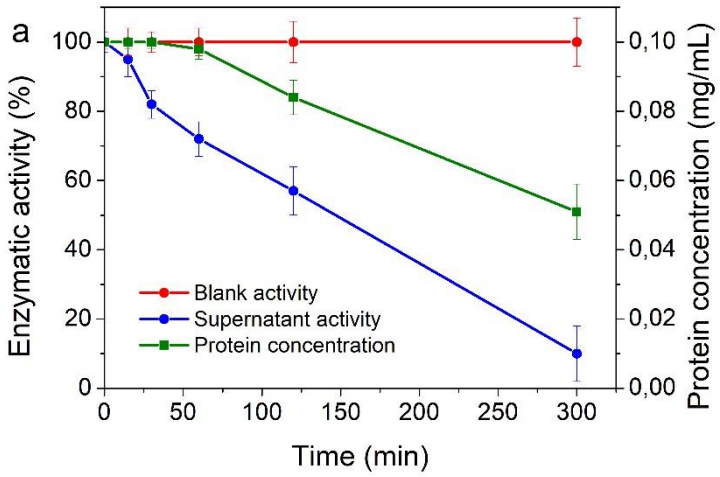

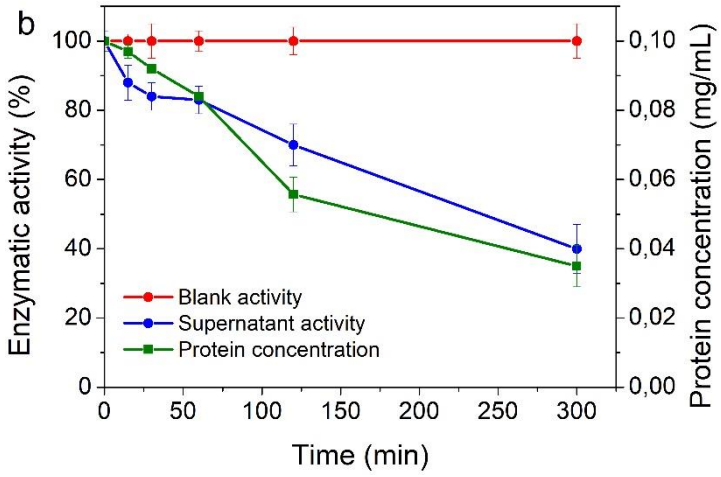

Figure 4 – Immobilization kinetics of FDH on (a) Z_G and (b) Z_A

To evaluate the immobilization, the various methods were evaluated based on IY and R_{act} expressed by the biocatalyst. In all immobilization tests, 1 g of support was contacted with 2 mg of FDH. The results obtained are reported in table 2. In all cases where the zeolite was milled before immobilization (tests 3, 4, 7 and 8), there was an increase of the IY with respect to the non-milled supports. This is attributed to the higher contact that the protein has to the surface of the internal pores of the particle. In addition, when a milling support is used, there is a reduction of the problem of pore blocking that the same protein can caused, when the enzyme is immobilized near of the entrance of the pores. Contrary to the results of IY, R_{act} values were higher in non-milled zeolite samples. It is worth to mention, that the measurement of enzymatic activity of the samples of the tests 1, 2, 5 and 6 was carried out on the samples milled after the immobilization process. Without the milling process after immobilization, in fact, these samples do not show activity in the time determined for the activity tests (120 s). This evidenced the presence of mixing problems inside the reaction medium and the necessity of performing a milling process after immobilization. As observed in literature, the internal diffusional restriction (IDR) depends on the particle size. As the size increases, the IDR increases and the activity decreases [46]. Thus, the difference on R_{act} cannot be attributed to the size of the particles used in the activity measurements. Probably, since the IYs assets are smaller, there are less mass transfer limitations and sodium formate can arrive to the enzymes that are immobilized deeper into the pore pores. When instead the immobilization yield reaches 100%, the pore is completely occluded, thus preventing the passage of formate molecules and thus lowering the activity. This supposition is in line with results reported by Suarez et al., where the authors demonstrated that the internal diffusional restriction (IDR) depends on the amount of enzyme loading; as the amount of enzyme increases, the IDR increases [46].

By comparing the two covalent immobilization strategies, the two-step strategy (Z_A) yields to higher IY (65 % with Z_A and 100 % with $Z_{A,m}$) in comparison with those obtained with Z_G (49 % with Z_G and 76% with $Z_{G,m}$). The results of IY are in line with those reported in literature with amino agarose (100 %) and glyoxyl agarose (50% to 100%) [16,47] and glyoxyl silica (75 %) [48]. In the case of R_{act}, the highest value was obtained with Z_G, which is the opposite as that reported in literature. For instance, Bolivar et al. reported a retained activity of 50 % and 30 % for amino agarose cross-linked with glutaraldehyde and glyoxyl agarose supports, respectively [16]. This result is attributed to the high value of IY obtained with Z_A, which could yield to higher IDR with respect to the Z_G sample. Furthermore, crosslinking with glutaraldehyde could result in high stiffness of the immobilized protein, which reportedly with other enzymes, reduces retained activity [19].

Table 2 - Immobilization yield (IY) and Retained activity (R_{act}) for the different FDH derivates.

Test	Support	Immobilization pH	IY [%]	R_{act} [%]
1	Z	7	100	9
2	Z_A	7	65	26
3	Z_m	7	100	5
4	$Z_{A,m}$	7	100	4
5	Z	10	86	28
6	Z_G	10	49	40
7	Z_m	10	95	14
8	$Z_{G,m}$	10	76	14

3.4 Thermal stability

To evaluate thermal stability, the biocatalysts made of FDH immobilized on Z_G and Z_A and the free enzyme were incubated at 50 °C. The residual activity in function of time is shown in Fig. 5. The solid lines were obtained by interpolating the experimental data by using a first order deactivation model with no residual activity for the free enzyme (Eq. 4) and a first order deactivation model with residual activity (Eq. 5) for the immobilized FDH. From those models it was therefore possible to obtain the inactivation kinetic parameters, like the deactivation constant (k_D), the half-life time ($t_{1/2}$) and the stabilization factor (F_S) [34]. The results are summarized in the table 3.

The free enzyme lost about 62 % of its initial activity after 24 h and no more activity was present after 48 h, whereas both the two biocatalyst samples, still showed activities above 50 % of the initial activity after 96 h. A similar stabilization factor was obtained with Z_G (14.8) and Z_A (18.9), as reported in table 3. This result is in line with the F_S values reported in literature, which varies from 4 with FDH CLEAs [49] to 150 with a FDH immobilized on glyoxyl-agarose [16]. The immobilization conditions of time and temperature could be optimized to have a further increment in the F_S.

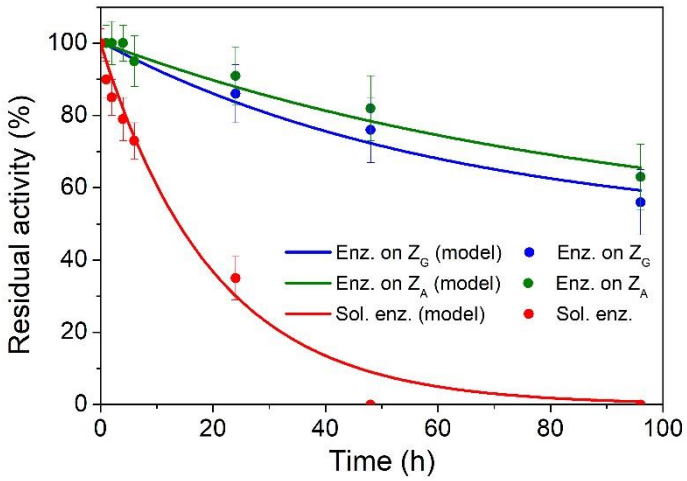

Figure 5 - Thermal stability at 50 °C for FDH immobilized on Z_G and Z_A and free FDH.

Table 3 – Inactivation kinetic parameters of the FDH derivates at 50 ºC by using a first order deactivation model with no residual activity for the free enzyme and with residual activity for the immobilized FDH samples.

Sample	k_D (h^{-1})	α	$t_{1/2}$ (h)	F_S	R^2
Free FDH	0.05	-	13.8	-	0.99
FDH on Z_G	0.016	0.48	203.6	14.8	0.97
FDH on Z_A	0.011	0.47	261.1	18.9	0.96

3.5 Effect of pH and temperature on FDH activity

The optimal pH study was carried out on Z_G and Z_A, in both cases the immobilization was carried out on the unground zeolite. In Fig. 6-a it was possible to see how the optimal pH varied for the

free enzyme and the two biocatalyst samples. In the case of FDH immobilized on Z_G, the optimal pH did not differ from that of the soluble enzyme. For the enzyme immobilized on Z_A, there was a shift of the maximum at higher pH. Probably inside the micropores of Z_A, due to the surface amino groups, a microenvironment with a different pH than that of the bulk was created, as also observed by Ottone et al. [50] in a agarose support with amino groups. Fig. 6-b shows similar trends of the temperature profile for the three cases with the same optimal temperature. This indicates that the structure of the enzyme surrounding the active site did not change during immobilization [22]. Moreover, at 60 °C in both immobilized enzyme samples the percentage activity is higher than that of the free enzyme, since the immobilization allows a greater stability and decreasing denaturation of the enzyme inside the microenvironment. Furthermore, in the 40 - 60 °C range, the fall in activity from the maximum value is less marked.

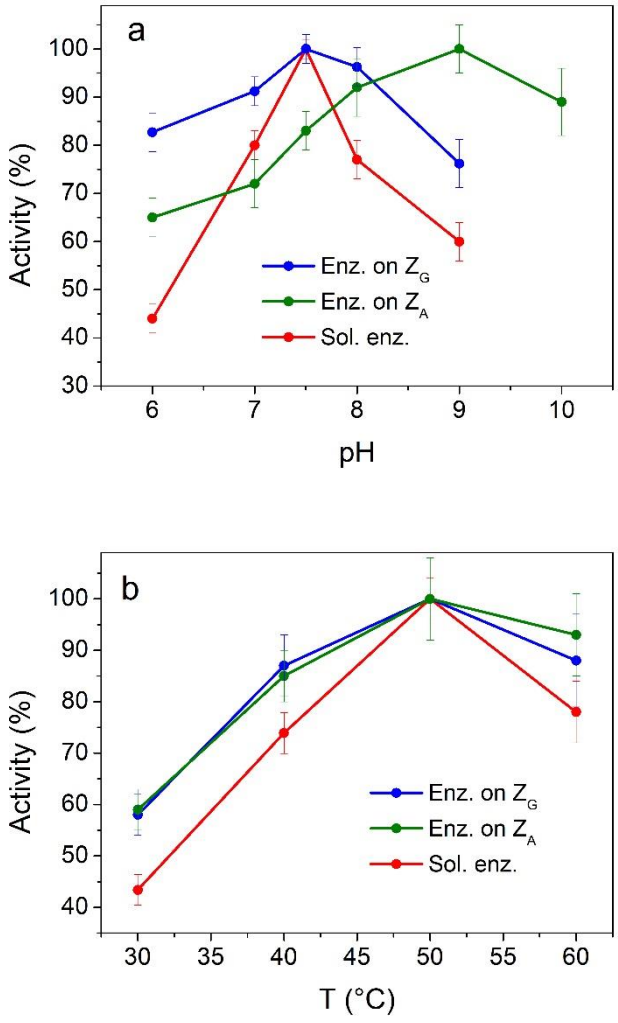

Figure 6 – Optimum pH (a) and T (b) for FDH immobilized on Z_G and Z_A and free FDH

3.6 Reaction of CO_2 reduction

The CO_2 reduction reaction was carried out in a sealed glass bottle and for the duration of the test CO_2 was blown in solution. A neutral pH was used to avoid NADH oxidation phenomena at more basic pH [51]. Even if the highest activity was observed at 50 ºC, the reaction was carried out at room temperature and atmospheric pressure. Highest temperatures have the drawback of reducing substantially the CO_2 concentration in aqueous media [52].

In both cases, 1 g of support with immobilized FDH was used. The specific activity of FDH on Z_G was 3.54 ± 0.1 IU/$g_{support}$, and on Z_A was 3.2 ± 0.1 IU/$g_{support}$.

Figure 7 shows the reaction kinetics of NADH consumption and formic acid production. The conversion of NADH was 37 % with Z_A and 34.6 % with Z_G. The production of formic acid was in accordance with the NADH consumed during the CO_2 reduction reaction. FDH immobilized both on Z_G and Z_A showed similar performance. The lowest NADH concentration (maximum conversion) was obtained at 45 minutes with Z_G and 90 minutes with Z_A. After that time and up to the end of the reaction, there was an increase of NADH concentration of about 30 % with Z_G and 10 % with Z_A. This phenomenon was attributed to the reverse reaction of oxidation of formic acid to CO_2, which is also catalyzed by FDH. In literature it was reported that the oxidation reaction is thermodynamically favored with respect to the reduction reaction [9]. Thus, at the beginning of the reaction, where no NAD^+ was present in the reaction media, only the reduced reaction was carried out. After 45 min, the NAD^+ concentration increased (minimum value of NADH) and the undesired reverse reaction occurred, in a lower proportion. The results are in line with those obtained by Kim et al. with free FDH from *Candida boidinii* (28% conversion referred to NADH, at pH 7 and 25 °C) [53]. Thus, covalently immobilized enzymes show no decrease in CO_2 reduction compared to the free enzyme and have the advantage of the reusability.

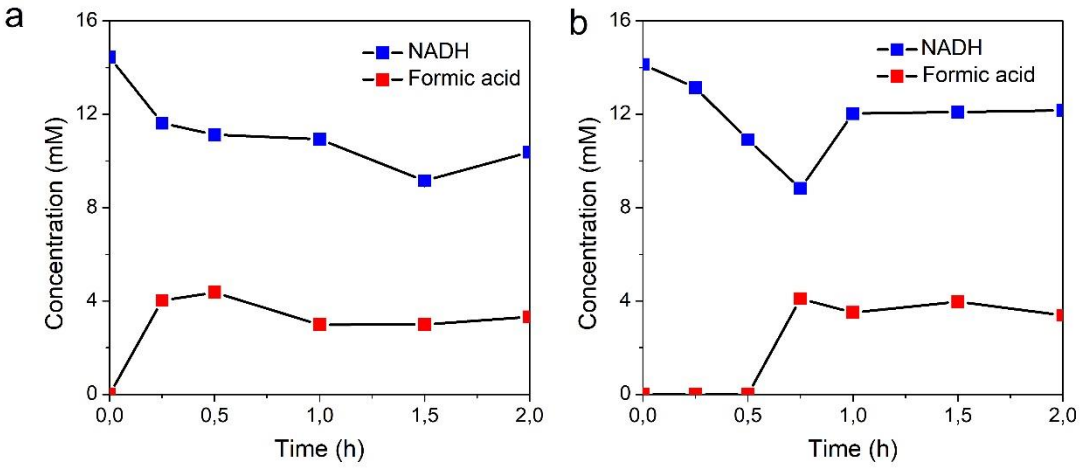

Figure 7 – Reaction kinetics of NADH consumption and formic acid production with FDH from *C. boidinii* on Z_A (a) and on Z_G (b).

3.6 Reusability of the immobilized FDH

The reusability of the biocatalysts was studied by performing repeated batch reactions. These tests were performed by using $NaHCO_3$ instead of CO_2 to simulate the reaction conditions. The concentration of $NaHCO_3$ used (34 mM) was equivalent to that which would be obtained with CO_2 at equilibrium according to Henry's law ($K_H = 3.39 \cdot 10^{-2}\ mol \cdot L^{-1} \cdot P^{-1}$) [52]. After 8 cycles the residual activity was constant near to 100%, see Fig. 8. From cycle 8 there was a decrease in activity in both cases, more noticeable with the FDH on Z_A. After 12 cycles, with FDH on Z_A there is a residual activity of 22% while with FDH on Z_G there is a residual activity of 80%. The stability observed during the first cycles was attributed to IDR. During the first cycles, the substrate reacted faster with the enzymes located on the outside of the zeolite channels, but over time the enzymes lost activity and the substrate was accessible to the enzymes immobilized in the deeper areas of the channels. A similar behavior was reported for alcohol dehydrogenase [50]. This result confirms that the highest IDRs were obtained with the Z_A than with the Z_G. Alagoz et al. reported a 60 % of residual activity after 10 cycles of use by using a FDH immobilized on glyoxyl silica [48]. By using other immobilization methods, such as CLEAs [49] or encapsulation [54], no loss of activity was observed after 10 cycles.

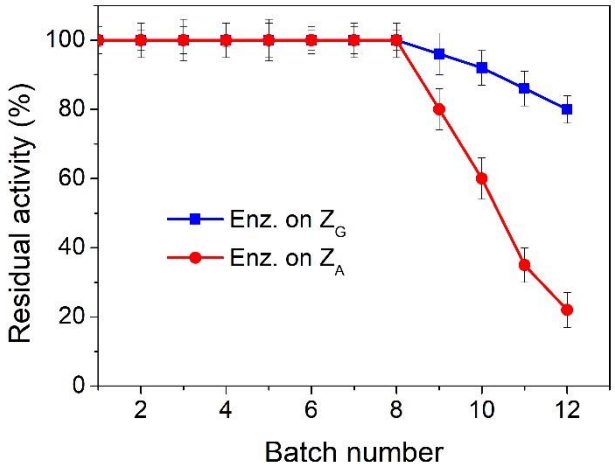

Figure 8 - Reuse test of FDH immobilized on Z_A and Z_G

4 Conclusions

The enzymatic conversion of CO_2 to formic acid was evaluated with FDH from *Candida boidinii* immobilized on natural zeolite by two different covalent immobilization methods.

FESEM and XRD analyses were carried out on the support, highlighting that the zeolite used corresponds to mordenite. Through the FTIR and BET analyses it was measured how the physical properties of the support changed after functionalization.

FDH was covalently immobilized on zeolite functionalized with glyoxyl (Z_G) or amino (Z_A) groups with glutaraldehyde cross-linking. This work reports for the first time the immobilization of FDH on zeolite support. The activity of the immobilized enzyme, compared to that of the free enzyme, was characterized as a function of pH and temperature. According to the pH tests, the Z_A sample showed a higher optimal pH (pH 9) with respect to the free enzyme and Z_G sample (pH 7.5). With regard to temperature, a similar trend was obtained with the immobilized and the free enzyme derivates, being the optimal temperature equal to 50 ºC. From the stability test performed at 50ºC, a F_S of ~15 and ~19 with the Z_G and the Z_A supports, respectively, was calculated. Finally, the two systems were studied on the CO_2 reduction reaction, obtaining conversion yields equal to 34.6 % with Z_G and 37 % with Z_A. Both biocatalysts can be used for at least 8 cycles without loss of activity, making them very interesting for the development of a continuous process.

To work continuously and to avoid reverse reaction, it would be necessary to implement a NADH regeneration system. To increase the CO_2 conversion yields, the procedure developed in this work can be replicated with FDH from other sources. In conclusion, this study shows a low-cost support option to obtain stable biocatalysts for the first step of a multi-enzymatic approach to produce molecules with a higher added value such as methanol.

Declaration of Competing Interest

The authors declare there is no conflict of interest

Acknowledgement

The authors thank FONDECYT Grant Number 11180967 for the financial support and the project "VALPO4CIRCULAR ECONOMY" funded by Compagnia San Paolo and Politecnico di Torino for the support of the internationalization of the research. The authors would also thank Lesly Chamorro and Mariela Muñoz for the analytical measurements of HPLC samples.

References

[1] NOOA, ESRL Global Monitoring Division - Global Greenhouse Gas Reference Network, (2016). https://www.esrl.noaa.gov/gmd/ccgg/trends/.

[2] A.M. Appel, J.E. Bercaw, A.B. Bocarsly, H. Dobbek, D.L. Dubois, M. Dupuis, J.G. Ferry, E. Fujita, R. Hille, P.J.A. Kenis, C.A. Kerfeld, R.H. Morris, C.H.F. Peden, A.R. Portis, S.W. Ragsdale, T.B. Rauchfuss, J.N.H. Reek, L.C. Seefeldt, R.K. Thauer, G.L. Waldrop, Frontiers, opportunities, and challenges in biochemical and chemical catalysis of CO_2 fixation, Chem. Rev. 113 (2013) 6621–6658. https://doi.org/10.1021/cr300463y.

[3] M. Aresta, A. Dibenedetto, Utilisation of CO_2 as a chemical feedstock: Opportunities and challenges, Dalt. Trans. 28 (2007) 2975–2992. https://doi.org/10.1039/b700658f.

[4] Celbicon Project, Cost-effective CO_2 conversion into chemicals via combination of Capture, ELectrochemical and BI-ochemical CONversion technologies, (2016). https://cordis.europa.eu/project/rcn/200178/factsheet/en.

[5] P.R. Yaashikaa, P. Senthil Kumar, S.J. Varjani, A. Saravanan, A review on photochemical, biochemical and electrochemical transformation of CO_2 into value-added products, J. CO_2 Util. 33 (2019) 131–147. https://doi.org/10.1016/j.jcou.2019.05.017.

[6] S. Bajracharya, S. Srikanth, G. Mohanakrishna, R. Zacharia, D.P. Strik, D. Pant, Biotransformation of carbon dioxide in bioelectrochemical systems: State of the art and future prospects, J. Power Sources. 356 (2017) 256–273. https://doi.org/10.1016/j.jpowsour.2017.04.024.

[7] R. Obert, B.C. Dave, Enzymatic Conversion of Carbon Dioxide to Methanol: Enhanced Methanol Production in Silica Sol-Gel Matrices, Ind. Eng. Chem. Res. 37 (1998) 12192–12193. https://doi.org/10.1021/ja991899r.

[8] J. Luo, A.S. Meyer, R. V. Mateiu, M. Pinelo, Cascade catalysis in membranes with enzyme immobilization for multi-enzymatic conversion of CO_2 to methanol, N. Biotechnol. 32 (2015) 319–327. https://doi.org/10.1016/j.nbt.2015.02.006.

[9] F. Marpani, M. Pinelo, A.S. Meyer, Enzymatic conversion of CO_2 to CH_3OH via reverse dehydrogenase cascade biocatalysis: Quantitative comparison of efficiencies of immobilized enzyme systems, Biochem. Eng. J. 127 (2017) 217–228. https://doi.org/10.1016/j.bej.2017.08.011.

[10] Y. Amao, Formate dehydrogenase for CO_2 utilization and its application, J. CO_2 Util. 26 (2018) 623–641. https://doi.org/10.1016/j.jcou.2018.06.022.

[11] A. Dibenedetto, P. Stufano, W. Macyk, T. Baran, C. Fragale, M. Costa, M. Aresta, Hybrid technologies for an enhanced carbon recycling based on the enzymatic reduction of CO_2 to methanol in water: Chemical and photochemical NADH regeneration, ChemSusChem. 5 (2012) 373–378. https://doi.org/10.1002/cssc.201100484.

[12] H. Song, C. Ma, P. Liu, C. You, J. Lin, Z. Zhu, A hybrid CO_2 electroreduction system mediated by enzyme-cofactor conjugates coupled with Cu nanoparticle-catalyzed cofactor regeneration, J. CO_2 Util. 34 (2019) 568–575. https://doi.org/10.1016/j.jcou.2019.08.007.

[13] H. Choe, J.C. Joo, D.H. Cho, M.H. Kim, S.H. Lee, K.D. Jung, Y.H. Kim, Efficient CO_2-reducing activity of NAD-dependent formate dehydrogenase from *Thiobacillus* sp. KNK65MA for formate production from CO_2 gas, PLoS One. 9 (2014). https://doi.org/10.1371/journal.pone.0103111.

[14] A.E. Alvarenga, M.J. Amoroso, A. Illanes, G.R. Castro, Cross-linked α-l-rhamnosidase aggregates with potential application in food industry, Eur. Food Res. Technol. 238 (2014) 797–801. https://doi.org/10.1007/s00217-014-2157-4.

[15] P. Zucca, E. Sanjust, Inorganic materials as supports for covalent enzyme immobilization: Methods and mechanisms, Molecules. 19 (2014) 14139–14194. https://doi.org/10.3390/molecules190914139.

[16] J.M. Bolivar, L. Wilson, S.A. Ferrarotti, R. Fernandez-Lafuente, J.M. Guisan, C. Mateo, Evaluation of different immobilization strategies to prepare an industrial biocatalyst of formate dehydrogenase from *Candida boidinii*, Enzyme Microb. Technol. 40 (2007) 540–546. https://doi.org/10.1016/j.enzmictec.2006.05.009.

[17] F. López-Gallego, L. Betancor, C. Mateo, A. Hidalgo, N. Alonso-Morales, G. Dellamora-Ortiz, J.M. Guisán, R. Fernández-Lafuente, Enzyme stabilization by glutaraldehyde crosslinking of adsorbed proteins on aminated supports, J. Biotechnol. 119 (2005) 70–75. https://doi.org/10.1016/j.jbiotec.2005.05.021.

[18] R. Fernández-Lafuente, V. Rodríguez, C. Mateo, G. Penzol, O. Hernández-Justiz, G. Irazoqui, A. Villarino, K. Ovsejevi, F. Batista, J.M. Guisán, Stabilization of multimeric enzymes via immobilization and post-immobilization techniques, J. Mol. Catal. B Enzym. 7 (1999) 181–189. https://doi.org/10.1016/S1381-1177(99)00028-4.

[19] I. Migneault, C. Dartiguenave, M.J. Bertrand, K.C. Waldron, Glutaraldehyde: Behavior in aqueous solution, reaction with proteins, and application to enzyme crosslinking, Biotechniques. 37 (2004) 790–802. https://doi.org/10.2144/04375rv01.

[20] J.M. Bolivar, L. Wilson, S.A. Ferrarotti, J.M. Guisán, R. Fernández-Lafuente, C. Mateo, Improvement of the stability of alcohol dehydrogenase by covalent immobilization on glyoxyl-agarose, J. Biotechnol. 125 (2006) 85–94. https://doi.org/10.1016/j.jbiotec.2006.01.028.

[21] D.S. Rodrigues, A.A. Mendes, W.S. Adriano, L.R.B. Gonçalves, R.L.C. Giordano, Multipoint covalent immobilization of microbial lipase on chitosan and agarose activated by different methods, J. Mol. Catal. B Enzym. 51 (2008) 100–109. https://doi.org/10.1016/j.molcatb.2007.11.016.

[22] C. Bernal, L. Sierra, M. Mesa, Improvement of thermal stability of β-galactosidase from *Bacillus circulans* by multipoint covalent immobilization in hierarchical macro-mesoporous silica, J. Mol. Catal. B Enzym. 84 (2012) 166–172. https://doi.org/10.1016/j.molcatb.2012.05.023.

[23] S. Mitchell, J. Pérez-Ramírez, Mesoporous zeolites as enzyme carriers: Synthesis, characterization, and application in biocatalysis, Catal. Today. 168 (2011) 28–37. https://doi.org/10.1016/j.cattod.2010.10.058.

[24] F. Yagiz, D. Kazan, A.N. Akin, Biodiesel production from waste oils by using lipase immobilized on hydrotalcite and zeolites, Chem. Eng. J. 134 (2007) 262–267. https://doi.org/10.1016/j.cej.2007.03.041.

[25] B. Liu, R. Hu, J. Deng, Characterization of Immobilization of an Enzyme in a Modified Y Zeolite Matrix and Its Application to an Amperometric Glucose Biosensor, Anal. Chem. 69 (1997) 2343–2348. https://doi.org/10.1021/ac960930u.

[26] C.S. Cundy, P.A. Cox, The hydrothermal synthesis of zeolites: Precursors, intermediates and reaction mechanism, Microporous Mesoporous Mater. 82 (2005) 1–78. https://doi.org/10.1016/j.micromeso.2005.02.016.

[27] X. Querol, N. Moreno, J.C. Umaa, A. Alastuey, E. Hernández, A. López-Soler, F. Plana, Synthesis of zeolites from coal fly ash: an overview, Int. J. Coal Geol. 50 (2002) 413–423. https://doi.org/10.1016/S0166-5162(02)00124-6.

[28] M.M. Bradford, A rapid and sensitive method for the quantitation of microgram quantities of protein utilizing the principle of protein-dye binding, Anal. Biochem. 72 (1976) 248–254. https://doi.org/10.1016/0003-2697(76)90527-3.

[29] J.M. Guisán, Aldehyde-agarose gels as activated supports for immobilization-stabilization of enzymes, Enzyme Microb. Technol. 10 (1988) 375–382. https://doi.org/10.1016/0141-0229(88)90018-X.

[30] P. Vejayakumaran, I.A. Rahman, C.S. Sipaut, J. Ismail, C.K. Chee, Structural and thermal characterizations of silica nanoparticles grafted with pendant maleimide and epoxide groups, J. Colloid Interface Sci. 328 (2008) 81–91. https://doi.org/10.1016/j.jcis.2008.08.054.

[31] H.P. Erickson, Size and shape of protein molecules at the nanometer level determined by sedimentation, gel filtration, and electron microscopy, Biol. Proced. Online. 11 (2009) 32–51. https://doi.org/10.1007/s12575-009-9008-x.

[32] J.M. Bolivar, J. Rocha-Martin, C. Mateo, F. Cava, J. Berenguer, R. Fernandez-Lafuente, J.M. Guisan, Coating of soluble and immobilized enzymes with ionic polymers: Full stabilization of the quaternary structure of multimeric enzymes, Biomacromolecules. 10 (2009) 742–747. https://doi.org/10.1021/bm801162e.

[33] L. Tavernini, C. Ottone, A. Illanes, L. Wilson, Entrapment of enzyme aggregates in chitosan beads for aroma release in white wines, Int. J. Biol. Macromol. 154 (2020) 1082–1090. https://doi.org/10.1016/j.ijbiomac.2020.03.031.

[34] A. Illanes, Enzyme biocatalysis: Principles and applications, Springer, 2008. https://doi.org/10.1007/978-1-4020-8361-7.

[35] H. Schutte, J. Flossdorf, H. Sahm, M.-R. Kula, Purification and Properties of Formaldehyde Dehydrogenase and Formate Dehydrogenase from *Candida boidinii*, Eur. J. Biochem. 62 (1976) 151–160. https://doi.org/10.1111/j.1432-1033.1976.tb10108.x.

[36] J. Coates, Interpretation of Infrared Spectra, A Practical Approach, in: Encycl. Anal. Chem., John Wiley & Sons, Ltd, Chichester, UK, 2006. https://doi.org/10.1002/9780470027318.a5606.

[37] S.A.M. Hanim, N.A.N.N. Malek, Z. Ibrahim, Amine-functionalized, silver-exchanged zeolite NaY: Preparation, characterization and antibacterial activity, Appl. Surf. Sci. 360 (2016) 121–130. https://doi.org/10.1016/j.apsusc.2015.11.010.

[38] B. Tyagi, C.D. Chudasama, R. V. Jasra, Determination of structural modification in acid activated montmorillonite clay by FT-IR spectroscopy, Spectrochim. Acta Part A. 64 (2006) 273–278. https://doi.org/10.1016/j.saa.2005.07.018.

[39] S.K. Saxena, N. Viswanadham, Enhanced catalytic properties of mesoporous mordenite for benzylation of benzene with benzyl alcohol, Appl. Surf. Sci. 392 (2017) 384–390. https://doi.org/10.1016/j.apsusc.2016.09.062.

[40] M. Gougazeh, J.C. Buhl, Synthesis and characterization of zeolite A by hydrothermal transformation of natural Jordanian kaolin, J. Assoc. Arab Univ. Basic Appl. Sci. 15

(2014) 35–42. https://doi.org/10.1016/j.jaubas.2013.03.007.

[41] A. Ates, C. Hardacre, The effect of various treatment conditions on natural zeolites: Ion exchange, acidic, thermal and steam treatments, J. Colloid Interface Sci. 372 (2012) 130–140. https://doi.org/10.1016/j.jcis.2012.01.017.

[42] R. Barin, D. Biria, S. Rashid-Nadimi, M.A. Asadollahi, Enzymatic CO_2 reduction to formate by formate dehydrogenase from *Candida boidinii* coupling with direct electrochemical regeneration of NADH, J. CO_2 Util. 28 (2018) 117–125. https://doi.org/10.1016/j.jcou.2018.09.020.

[43] S.A.M. Hanim, N.A.N.N. Malek, Z. Ibrahim, Analyses of surface area, porosity, silver release and antibacterial activity of amine-functionalized, silver-exchanged zeolite NaY, Vacuum. 143 (2017) 344–347. https://doi.org/10.1016/j.vacuum.2017.06.038.

[44] J.M. Bolivar, F. López-Gallego, C. Godoy, D.S. Rodrigues, R.C. Rodrigues, P. Batalla, J. Rocha-Martín, C. Mateo, R.L.C. Giordano, J.M. Guisán, The presence of thiolated compounds allows the immobilization of enzymes on glyoxyl agarose at mild pH values: New strategies of stabilization by multipoint covalent attachment, Enzyme Microb. Technol. 45 (2009) 477–483. https://doi.org/10.1016/j.enzmictec.2009.09.001.

[45] M. Yoshimoto, T. Yamashita, T. Yamashiro, Stability and reactivity of liposome-encapsulated formate dehydrogenase and cofactor system in carbon dioxide gas-liquid flow, Biotechnol. Prog. 26 (2010) 1047–1053. https://doi.org/10.1002/btpr.409.

[46] S. Suárez, C. Guerrero, C. Vera, A. Illanes, Effect of particle size and enzyme load on the simultaneous reactions of lactose hydrolysis and transgalactosylation with glyoxyl-agarose immobilized β-galactosidase from *Aspergillus oryzae*, Process Biochem. 73 (2018) 56–64. https://doi.org/10.1016/j.procbio.2018.08.016.

[47] J.M. Bolivar, L. Wilson, S.A. Ferrarotti, R. Fernandez-Lafuente, J.M. Guisan, C. Mateo, Stabilization of a formate dehydrogenase by covalent immobilization on highly activated glyoxyl-agarose supports, Biomacromolecules. 7 (2006) 669–673. https://doi.org/10.1021/bm050947z.

[48] D. Alagöz, A. Çelik, D. YIldIrIm, S.S. Tükel, B. Binay, Covalent immobilization of *Candida methylica* formate dehydrogenase on short spacer arm aldehyde group containing supports, J. Mol. Catal. B Enzym. 130 (2016) 40–47. https://doi.org/10.1016/j.molcatb.2016.05.005.

[49] M.H. Kim, S. Park, Y.H. Kim, K. Won, S.H. Lee, Immobilization of formate dehydrogenase from *Candida boidinii* through cross-linked enzyme aggregates, J. Mol. Catal. B Enzym.

97 (2013) 209–214. https://doi.org/10.1016/j.molcatb.2013.08.020.

[50] C. Ottone, C. Bernal, N. Serna, A. Illanes, L. Wilson, Enhanced long-chain fatty alcohol oxidation by immobilization of alcohol dehydrogenase from *S. cerevisiae*, Appl. Microbiol. Biotechnol. 102 (2018) 237–247. https://doi.org/10.1007/s00253-017-8598-5.

[51] O.H. Lowry, J. V. Passonneau, M.K. Rock, The stability of pyridine nucleotides., J. Biol. Chem. 236 (1961) 2756–2759.

[52] R.H. Perry, D.W. Green, Perry's Chemical Engineers' Handbook, 8th Edition, McGraw-Hill, 2007.

[53] S. Kim, M.K. Kim, S.H. Lee, S. Yoon, K.D. Jung, Conversion of CO_2 to formate in an electroenzymatic cell using *Candida boidinii* formate dehydrogenase, J. Mol. Catal. B Enzym. 102 (2014) 9–15. https://doi.org/10.1016/j.molcatb.2014.01.007.

[54] F. Kurayama, S. Suzuki, N.M. Bahadur, T. Furusawa, H. Ota, M. Sato, N. Suzuki, Preparation of aminosilane-alginate hybrid microcapsules and their use for enzyme encapsulation, J. Mater. Chem. 22 (2012) 15405–15411. https://doi.org/10.1039/c2jm31792c.